PROCEEDINGS, 48th Workshop on Geothermal Reservoir Engineering
Stanford University, Stanford, California, February 6-8, 2023
SGP-TR-224

Thermal-Hydraulic-Mechanical (THM) Modeling of Fluid Flow and Heat/Tracer Transport Between Injection and Production Wells at the Utah FORGE Site

Robert Podgorney[1], Lynn Munday[1], Jerry Liu[1], Aleta Finnila[2], Branko Damjanac[3], Pengju Xing[3], and Zorica Radakovic-Guzina[3]

[1] Idaho National Laboratory, Idaho Falls, ID, USA

[2]WSP USA Inc., Redmond, WA, USA

[3]Itasca Consulting Group, Inc., Minneapolis, MN, USA

robert.podgorney@inl.gov

Keywords: FORGE, EGS, fracture flow

ABSTRACT

The Frontier Observatory for Research in Geothermal Energy (FORGE) site is a multi-year initiative funded by the U.S. Department of Energy for enhanced geothermal system research and development. The site is located on the margin of the Great Basin near the town of Milford, Utah. Modeling and simulation are playing a critical role at FORGE, being considered as a general scientific discovery tool to elucidate behavior of enhanced geothermal systems and as a deterministic (or stochastic) tool to plan and predict specific project activities.

In this analysis, we use the FALCON simulator to study mid-term flow and transport (6 month) in the enhanced geothermal system (EGS) reservoir focusing on the breakthrough times for injected tracers and thermal fronts, in an effort to provide input on injection-production well spacing that can ensure reliable and sustainable heat recovery from the geothermal reservoir over the testing timeframe of the FORGE program. An independent modeling of the same problem was carried out using XSite, the numerical model based on the lattice method, with the objective of increasing confidence in the model predictions.

A 3-dimensional Thermal-Hydraulic Mechanical (THM) reservoir model that encompasses the zones that were stimulated in Well 16, consisting of a 2.16e8 m^3 volume using grid cells that range from 2 to 100 m has been developed for the analysis. For selected cases, the reservoir model is coupled to a 1-dimensional thermal hydraulics simulation of non-isothermal fluid through Well 16, including perforations emplaced during the stimulation process. The combined simulation examines pressure and temperature changes (along with associated fluid property changes) in the well bore, partitions spatially and temporally varying flow exiting the well and entering the geothermal reservoir by examining the pressure difference between the perforated zones in the well and the surrounding formation and the reservoir along with the reservoir permeability, and assigns three point sources in the reservoir model that correspond to the three stimulation zones in the well. Spatial and temporal evolution of the fractured permeability in the reservoir resulting from injecting cold fluid (50°C) into the initially hot reservoir (~220°C) results in both poro-elastic and thermo-elastic evolution of the reservoir.

For this simulation, the location of the production well was situated directly above the injection well, vertically offset by three distances (75 m, 100 m and 125 m) to examine tracer the thermal breakthrough times. An open hole completion of the production well (Well 16B) was simulated using the formulation by Peaceman, where the spatial variability of flow along the well bore could be evaluated. The extraction behavior shows an interesting response to the pressure and temperature evolution in the reservoir

1. INTRODUCTION

The Frontier Observatory for Research in Geothermal Energy (FORGE) is a multiyear, multiphase initiative funded by the U.S. Department of Energy (DOE) for testing targeted enhanced geothermal system (EGS) research and development. The site is located inside the southeast margin of the Great Basin near the town of Milford, Utah (Figure 1 and Figure 2). The FORGE initiative consisted of three phases, which can be generally described as initial site selection (Phase 1), site characterization and down-selection (Phase 2), and site establishment and operations (Phase 3).

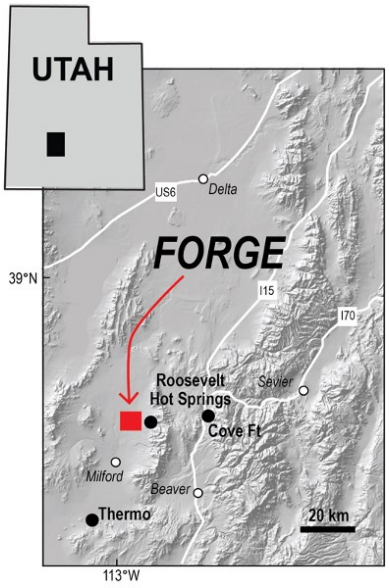

Figure 1. Location of FORGE site near Milford, Utah, USA.

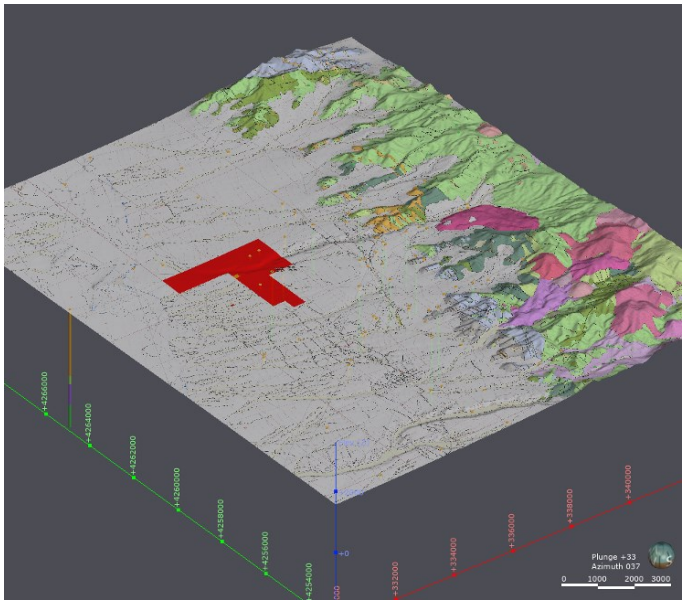

Figure 2. Location map of the Utah FORGE site (red highlighted area) and the earth model domain near Milford, Utah, with an oblique view showing the topography and the updated geologic map (Kirby, 2019).

The work to date at the Utah FORGE site has resulted in the compilation of a large amount of data within and surrounding the project site, incorporating information for Roosevelt Hot Springs, the central segment of the Mineral Mountains, and most of the north Milford Valley.

The current focus of site activities is on the design, drilling, and completion of Well 16B, the second deep, long offset well at the site. The modeling and simulation activities described in this paper were undertaken to inform the potential vertical offset between the existing Well 16A and the planned Well 16B.

1.1 Modeling and Simulation Overview

Multiphysics reservoir models have been developed to simulate the coupled thermo-hydro-mechanical responses in the subsurface to FORGE reservoir creation and operation activities. The numerical reservoir model used for this analysis is based on the reference native state numerical model of the reservoir (Liu at al., 2022; Podgorney et al., 2021). Continuum-based modeling codes are by far the most prevalent in geothermal reservoir engineering. Solution schemes based on finite-difference, finite-element, or finite-volume methods all

represent the subsurface as a generalized representative elementary volume, at various grid scales, to simulate and predict behavior. In densely fractured formations, it is common to use a discrete fracture network (DFN) as a starting point to develop upscaling relationships in the development of continuum models. For the current modeling effort, we use an interpreted DFN based on the results of stimulation activities carried out in April 2022, using FracMan (Golder Associates, 2019) and the FALCON code (Podgorney et al., 2014, ,Xia et al., 2016). The independent, alternative modeling of the same problem was carried out using XSite, the numerical code based on lattice model, with capability to simulate response of rock mass to fluid injection by explicitly modeling discrete fractures and potential fracture propagation.

FALCON (Fracturing And Liquid CONvection) is a geothermal reservoir simulation code developed using Idaho National Laboratory's (INL) Multiphysics Object-Oriented Simulation Environment (MOOSE) framework (Lindsay et al, 2022). It was written for the simulation of both conventional and enhanced geothermal reservoirs. The architecture that FALCON inherits from MOOSE has a plug-and-play modular design structure based on representing each piece of the residual term in a weak form of the governing partial differential equations (PDEs) as a "kernel." Kernels may be coupled together to achieve different application goals. All kernels are required to supply a residual, which usually involves summing products of finite-element shape functions. The basic architecture of the code allows convenient coupling of different processes. FALCON has been rigorously validated through a number of benchmark problems in Xia, Podgorney, and Huang (2016) and made available as an open-source toolkit (Xia and Podgorney, 2016).

XSite (Damjanac et al., 2020) is a three-dimensional hydraulic fracturing numerical simulation program based on the Synthetic Rock Mass (SRM) and the lattice methods. It is capable of modeling multiple wellbores with multiple stages and clusters, including open-hole completions and perforation tunnels. XSite resolves general hydraulic fracture propagation and interaction, including propagation in naturally fractured reservoirs with deterministically or stochastically generated DFNs. Interaction of hydraulic fractures with DFN can result in fluid leakoff and hydro-shearing of pre-existing fractures. The models conduct fully coupled thermo-hydro-mechanical simulations. Fluid flow is simulated as fracture flow within the joint networks and as matrix flow within the intact rock. The thermal model (Detournay et al., 2022) can simulate heat advection by fluid flowing in the fractures, joints, and forced heat convection at the rock-fluid interface, coupled with heat conduction in the rock and overall mechanical deformation.

1.2 April 2022 Stimulation Efforts

A stimulation campaign was carried out at the Utah FORGE site in April 2022. Three stages were stimulated. The locations of the three stages are illustrated in Figure 3. Stage 1 was conducted in the openhole section at the toe, and Stages 2 and 3 were conducted with perforation in the cased section. For Stage 1 and 2, slickwater was used while xlink gel was used in Stage 3. Table 1 summaries the pumping information for the three stages.

The stimulation was monitored by geophones in multiple offset wells. The detected microseismic events are shown in Figure 4.

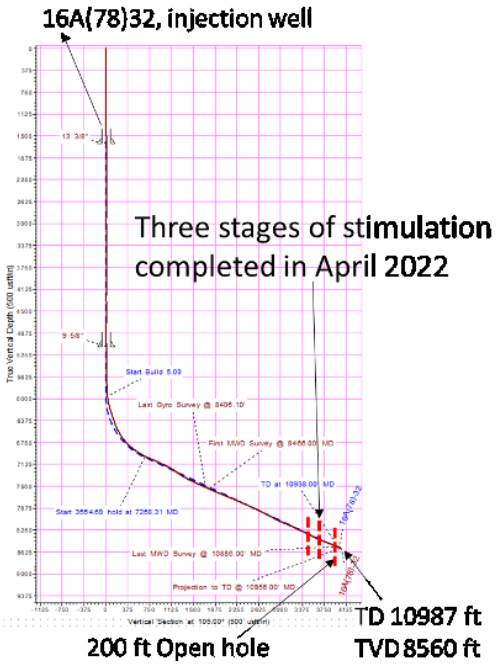

Figure 3. Location of the three stimulation stages in Well 16A.

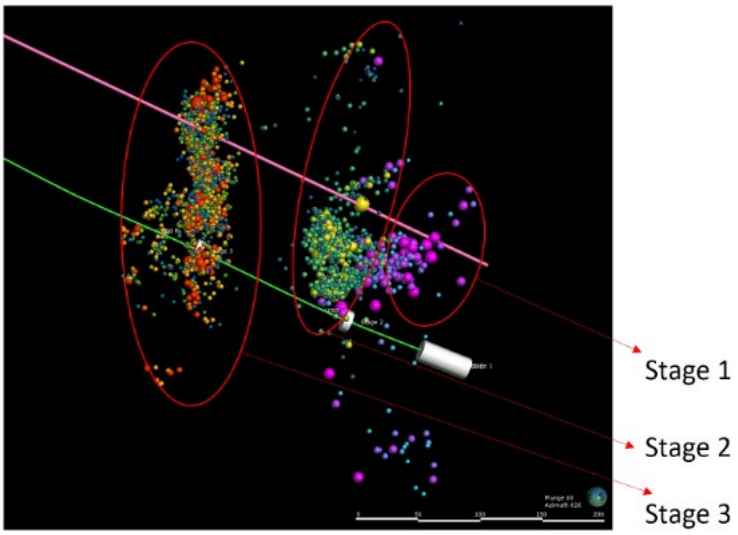

Figure 4. Microseismic event hypocenters for the three stimulation stages. Well 16A shown as green line, stimulation internals represented as gray cylinders. The magenta line is a potential Well 16B trajectory located 100m above 16A. Figure created by Hari Neupane at INL using Leapfrog Geothermal.

Table 1. Field pumping information for the three stages stimulation

Stage No.	Pumping fluid	Maximum pumping rate (bpm)	Pumped volume (bbl)	Completion	TVD (ft)
1	Slickwater	50	4261	Openhole	8490
2	Slickwater	35	2777	Cased	8410
3	xlink gel	35	3016	Cased	8224

1.3 Interpretation of microseismic data

Earthquake catalogues for the three hydraulic stimulation stages of well 16A(78)-32 were used to create an updated DFN model intended to capture significant flow pathways post-stimulation (WSP Golder, 2022). Potential planar features representing faults or fractures were identified by visual inspection while rotating the MEQ point cloud in 3D (data available from University of Utah Seismograph Stations, 2022). **Figure 5** Additional planes were added to connect the features identified from the MEQ data as shown in Figure 5 based on previous fracture orientation characterization work (Finnila et al., 2021).

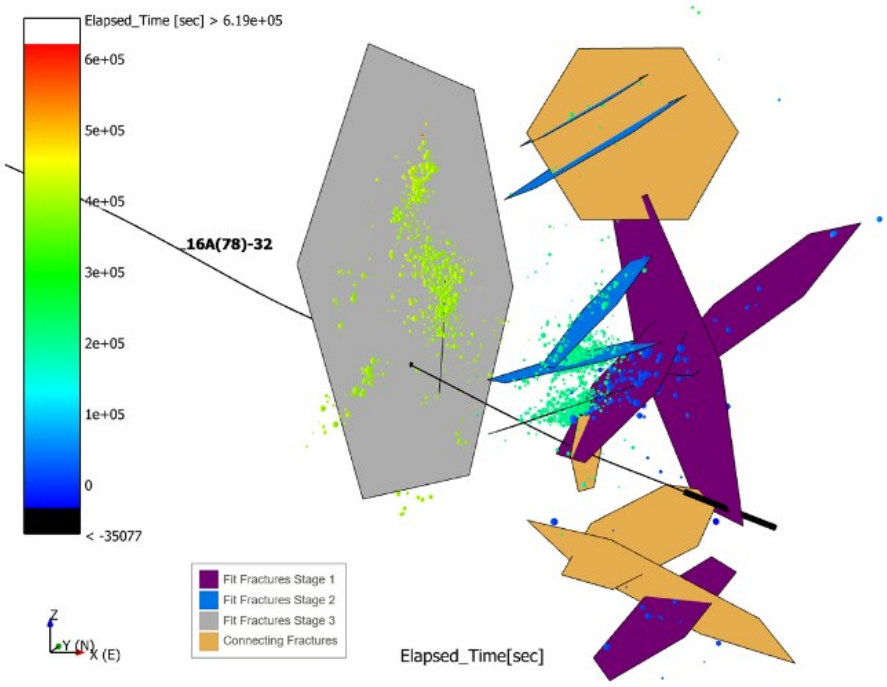

Figure 5: Side view of the fifteen fracture planes included in the updated reference Discrete Fracture Network model based on an interpretation of the preliminary earthquake catalog (MEQ) from the stimulation of well 16A(78)-32. MEQ shown as point data with color corresponding to elapsed time from the first measured event and sizes are scaled by the calculated moment magnitude.

2. FLOW AND TRANSPORT MODELING

Numerical models were developed for the geothermal reservoir in the fractured granitic rocks encompassing the volume of the FORGE subsurface interpreted to be affected by the April 2022 stimulation activities, and extending to the surrounding area to minimize interactions of the transient models with boundaries of the model domain.

As stated in the Inroduction, the modeling described in this paper were undertaken to better understand the spatial distribution of pressure, temperature, and stress and how it evolves during reservoir operations. The immediate use of the modeling results isto support site design decisions regarding the vertical offset between Well 16A and the soon to be drilled Well 16B. The offset between the wells, and the flow rates used during testing, will control the amount of time for both thermal and tracer breakthrough to occur during circulation testing at the site. The objective is to balance reservoir thermal sustainability with reasonable amounts of time to see measurable changes in the production fluid temperature and tracer concentrations.

As discussed in the following subsections, the fracture network interpreted to have been created during the April 2022 stimulation activities was directly used for flow and transport modeling. Note that current site development plans for 16B are envisioned to case and cement the fracture zone created during Stage 3 of the stimulation—therefore, the Stage 3 fracture zone is not included in this evaluation.

Willis and Podgorney (2023, *this issue*) presented a computational fluid dynamics (CFD) assessment of flow fluid and heat transport for injection into Well 16A, into and through the fractured reservoir, and production from Well 16B. The results of this analysis showed a high degree of sensitivity to the presence or absence of perforations in the production well, the number of effective perforations in the injection well, and the presence of an openhole toe section in Well 16A—showing that for most reasonable cases the openhole section will take 80 to 90% of the injected fluid. For this reason, a number of flow distribution cases were developed to examine the sensitivity of the production temperature and tracer breakthrough to injection well flow distributions. The CFD has been coupled to the reservoir models developed for this assessment, but the results are not presented here as the evaluation is on-going.

2.1 Model location and dimensions

The numerical model domain was sized to accommodate the geothermal reservoir intersected by the stimulated section of Well 16A and several production well offsets. A simulation domain 600 m × 600 m × 600 m, located approximately between depths of 2300 m to 3900 m below the surface, aligned with the calculated principal stress direction (N20E, see Figure 6 and Figure 7).

The discrete fractures were directly meshed (as intersecting 2-dimensional planes) in the model domain. An unstructured mesh with uniform 2 m spacing on the fractures and up to 100 m in the matrix was used, which resulted in approximately 2 million grid cells. Figure 7 shows a cutaway view of mesh along the trajectory of Well 16B, and illustrates the mesh density used to capture the hydro-thermal dynamics as fluid is injected and produced in through the reservoir.

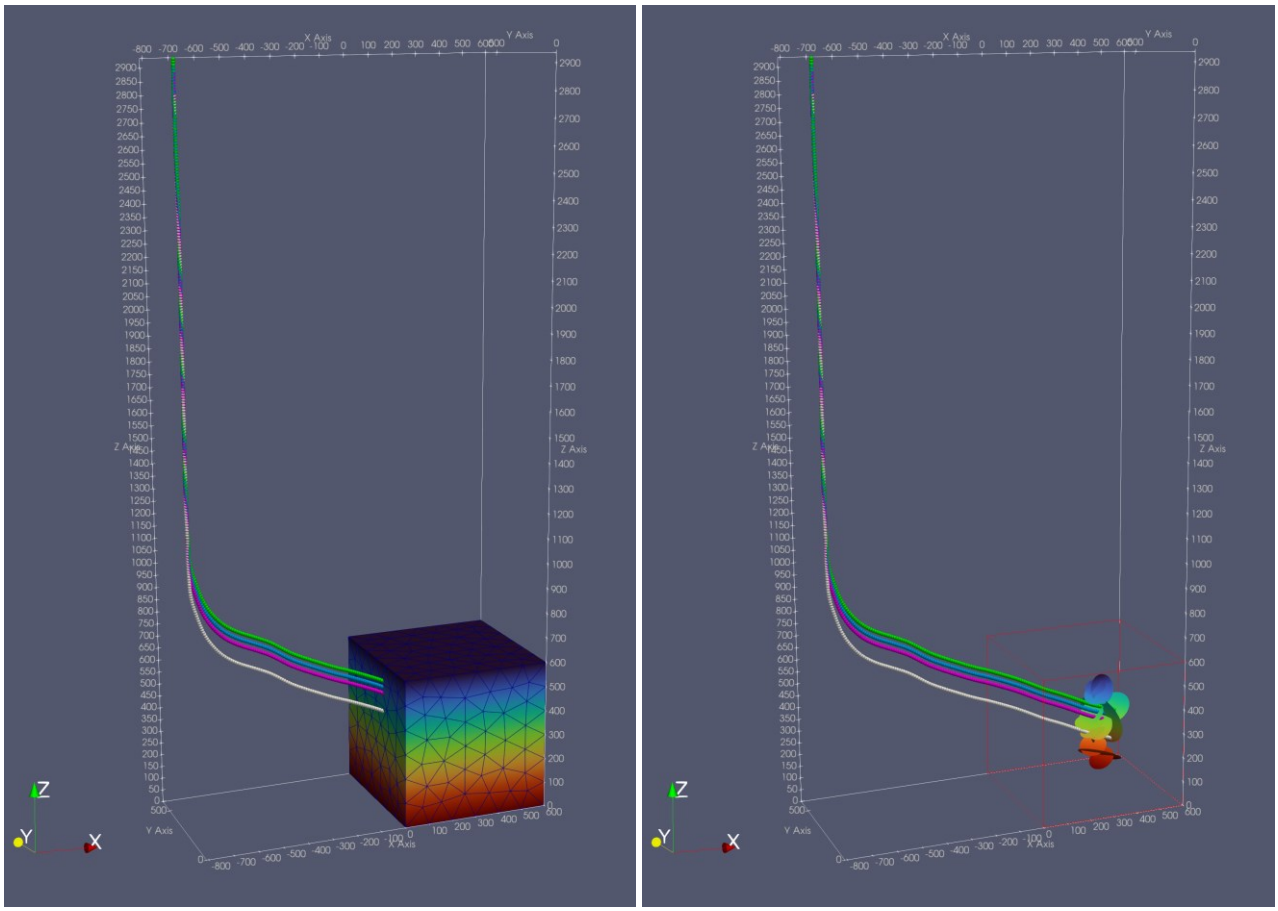

Figure 6. Numerical model domain colored cube, also showing Well 16A (gray line) and three potential offset distances for Well 16B (red = 75 m, blue = 100 m, and green = 125m separation). Left images shows the 600 m full model domain while the right image only shows the discrete fractures.

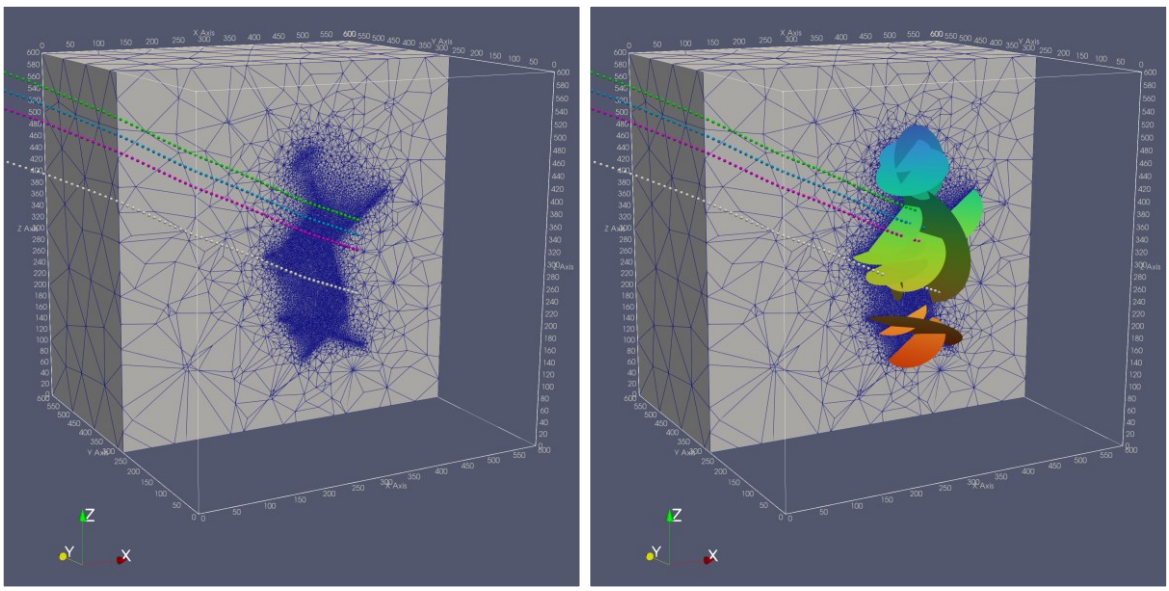

Figure 7. Cut-away of the numerical model domain, approximately along the path of Well 16B. Left image shows the mesh density in the matrix needed to capture the thermal interaction with the fractures, right image shows the fracture planes.

Figure 8 illustrates the complexity of the potential inflow and outflow zones within the injection and production wells. As stated above, only the open hole toe section and the first perforation zone are currently planned to be available for testing after the initial drilling of Well 16B. While 16A intersects the interpreted fractures from the April 2022 stimulation in 3-4 locations, only two are available for injection due to the locations where the open hole and perforations exist, these are identified with the red dots on Figure 8. To the contrary, initial confirmatory testing of the 16A-16B doublet is expected to have a significant open hole section near the toe of Well 16B, allowing for all zones intersected by the fractures created by the first two stimulation stages to be accessible.

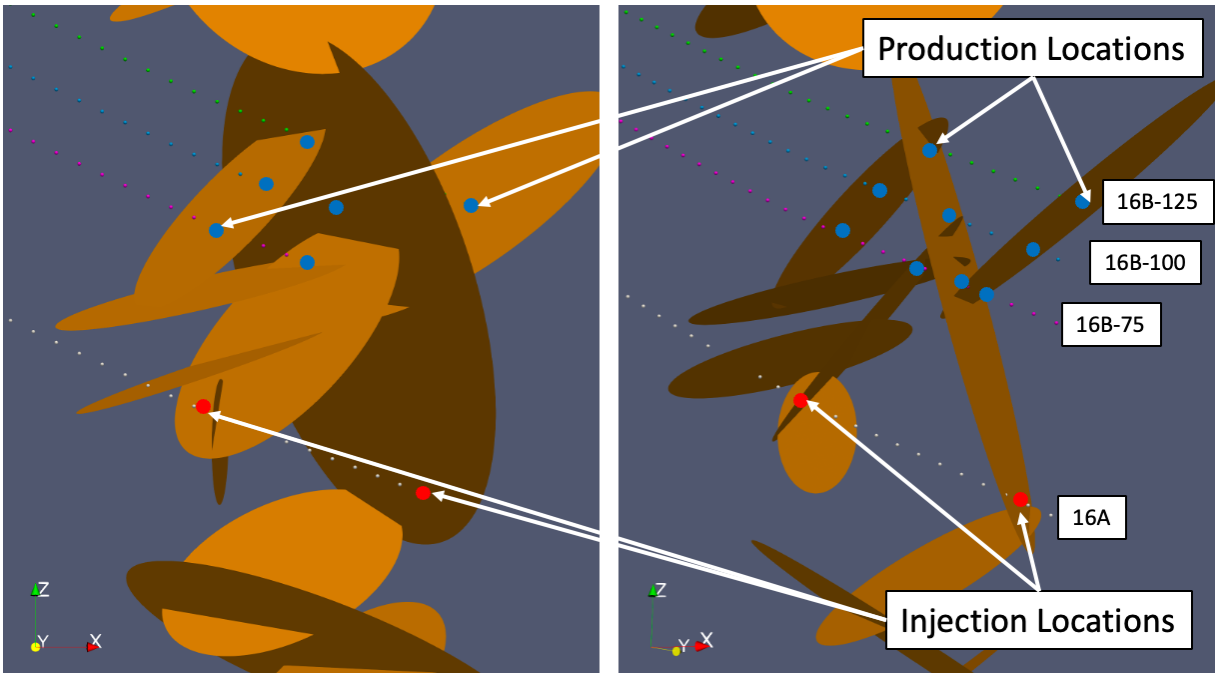

Figure 8. Close up image at two rotations of the discrete fractures, Well 16A (gray line) and three potential offset distances for Well 16B (red = 75 m, blue = 100 m, and green = 125m separation). Injection locations are highlighted with red dots, production locations with blue dots.

2.2 Boundary and initial conditions

Boundary conditions for pressure, temperature, and stress were based off the native state modeling results (Liu et al., 2022, Podgorney et al., 2021). Due to the complex nature of the distributions of pressure, temperature, and stress, all boundary conditions in the native state model had varying degrees of spatial variability, but at the scale of the model domain used for this analysis the variability was minimal. Therefore, uniform values were used. Specific boundary conditions and the values used will be discussed in detail in the following paragraphs.

Initial temperatures in the model region were predicted to be between 196.8°C at the top and 236.8°C at the bottom boundaries, while the pressure values ranged from 21 MPa to 27 MPa on the top and bottom boundaries, respectively. Boundary and initial conditions were based on results of native state modeling (Liu et al., 2022, Podgorney et al., 2021).

The top surface of the model domain was assigned a Dirichlet condition for pressure, all other boundaries of the model domain were assumed to be impermeable. While this assumption may not be perfectly valid, the model domain was chosen in order to omit the overlying sedimentary section as possible to avoid having to consider lateral flow originating from the outflow around the terminus of the Opal Mound Fault. The extremely low permeability of the granitoid justifies a no-flow condition

Temperature used a Dirichlet for both the top and bottom boundaries, with a linear interpolation applied internally for an initial condition. This is in general agreement with the native state model and conductive temperature profiles observed at the site.

In FALCON, stress is a derived quantity based on calculations of the displacement of the rock matrix. As such, it is difficult to assign a priori. A value of zero displacement was assigned as an initial condition, letting the model nonlinear solver iterations to come to a converged solution on the first time step.

Table 1. Reservoir and fracture properties used for the simulations (see Podgorney et al., 2021).

Parameter	Matrix Value	Fracture Value	Units
Permeability	1e-18	1e-12	m^2
Thermal conductivity	3.05	0.6e-4	W/m K
Porosity	0.001	0.9	--
Specific heat capacity	790	10	J/kg K
Young modulus	6.2e10	6.2e10	Pa
Bulk modulus	5.4e10	5.4e10	Pa
Rock grain density	2750	2700	Kg/m^3
Poisson's ratio	0.3	0.3	--
Biot coefficient	0.47	0.47	--

2.3 Operational scenarios

As discussed above, a CFD analysis for the flow dynamics within the injection well showed a high degree of sensitivity to pressure drop through perforation zones in Well 16A (Willis and Podgorney, 2023). Directly coupling a CFD solution scheme for well flow (Navier-Stokes equations) with reservoir flow (Darcy equations) is numerically challenging and computationally expensive. While this has been accomplished for the FORGE program, the analysis is on-going and incomplete and will be presented later. For these reasons, a series of nine modeling cases were developed to examine potential ranges in behavior for flow exiting well 16A and entering the EGS reservoir. With the exception of two cases, all had a total inflow of 10 kg/s, distributed among the two accessible inflow zones in Well 16B. Table 2 summarizes the cases. Based on Willis and Podgorney (2023), the most likely scenario is Case 1.

Table 2. Injection rates for the Openhole Zone and Perforation Zone 1 associated with the modeling cases used in the FALCON modeling.

Modeling Case	Open Hole Source Term (kg/sec)	Perforation Zone 1 Source Term (kg/sec)
1	9	1
2	7.5	2.5
3	5	5
4	2.5	7.5
5	1	9
6	5	0
7	10	0
8	0	5
9	0	10

In the XSite model it is assumed that 10 kg/s is injected in all three stages. The perforation pressure drop was not considered in Stages 2 and 3, but the model resolves distribution of injected flow rate between intersected fractures using approximation of flow along the well.

3.0 RESULTS

Results from both the FALCON and XSite simulations are presented below.

3.1 FALCON models

Figures 9-17 present thermal and injected fluid breakthrough curves for the 9 modeling cases. Each figure summarizes the 75, 100, and 125 m separation between Wells 16A and 16B. Unsurprisingly, the cases with larger well separation predict a longer amount of time for breakthrough, with injected fluid reaching Well 16B in appreciable quantities in as little as 7 days for the closest well separation.

Thermal breakthrough takes considerably longer in all cases, owing to the heat exchange between the fractures and the surrounding matrix. For the cases considered, the fastest initial thermal breakthough occurs after approximately 16-17 days, with the longest being over 50 days.

Figure 18 illustrates an example of the complexity of the heat structures that develop in the reservoir. It presents the temperature distribution in the fracture system after 6 months of injection for Case 1. The multiple flow paths between the injection and production points are clearly illustrated.

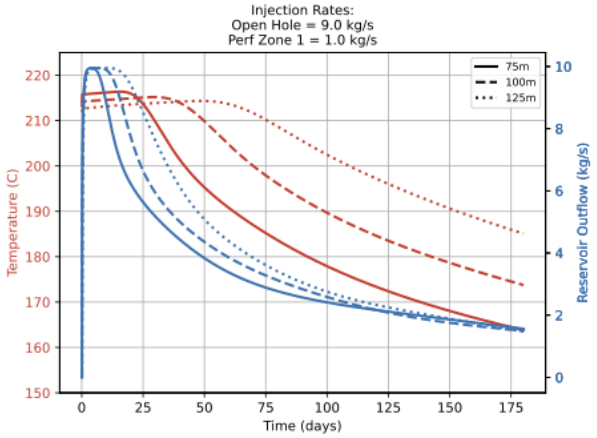

Figure 9. Numerical model results for Case 1. Red lines represent the simulated thermal breakthrough, while the blue lines represent the mass fraction of in-situ reservoir water produced corresponding to conservative fluid transport. The solid line represents the 75m well separation scenario, the long dash the 100m scenario, and the short dash the 125m separation scenario.

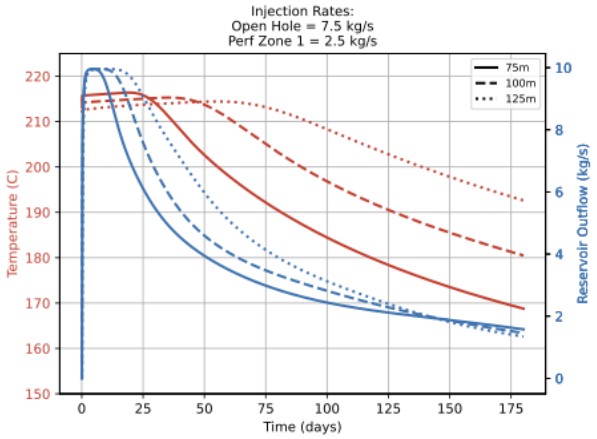

Figure 10. Numerical model results for Case 2. Red lines represent the simulated thermal breakthrough, while the blue lines represent the mass fraction of in-situ reservoir water produced corresponding to conservative fluid transport. The solid line represents the 75m well separation scenario, the long dash the 100m scenario, and the short dash the 125m separation scenario.

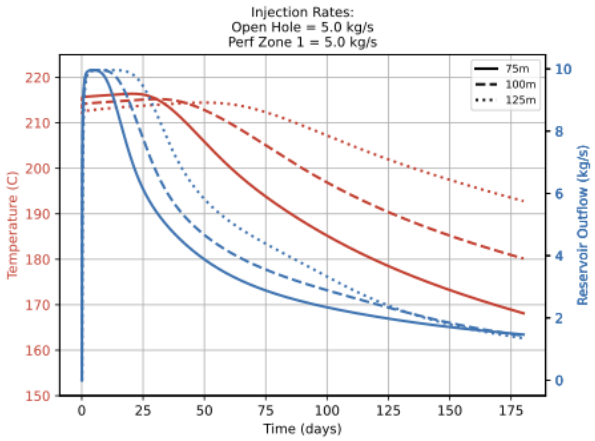

Figure 11. Numerical model results for Case 3. Red lines represent the simulated thermal breakthrough, while the blue lines represent the mass fraction of in-situ reservoir water produced corresponding to conservative fluid transport. The solid line represents the 75m well separation scenario, the long dash the 100m scenario, and the short dash the 125m separation scenario.

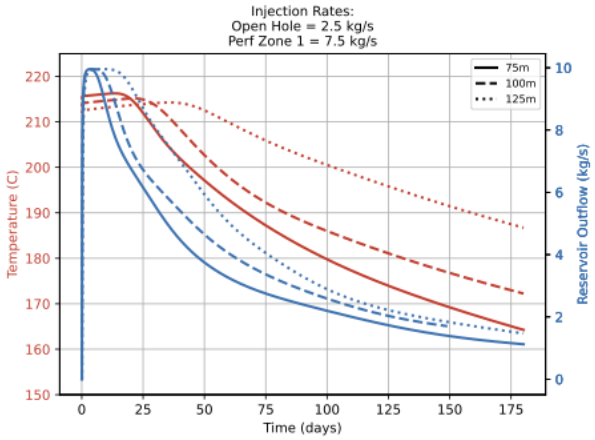

Figure 12. Numerical model results for Case 4. Red lines represent the simulated thermal breakthrough, while the blue lines represent the mass fraction of in-situ reservoir water produced corresponding to conservative fluid transport. The solid line represents the 75m well separation scenario, the long dash the 100m scenario, and the short dash the 125m separation scenario.

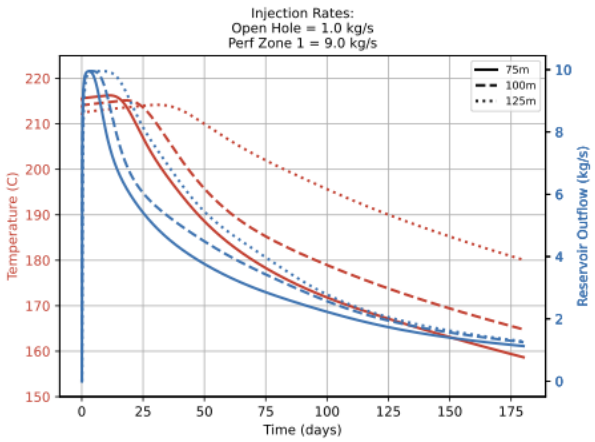

Figure 13. Numerical model results for Case 5. Red lines represent the simulated thermal breakthrough, while the blue lines represent the mass fraction of in-situ reservoir water produced corresponding to conservative fluid transport. The solid line represents the 75m well separation scenario, the long dash the 100m scenario, and the short dash the 125m separation scenario.

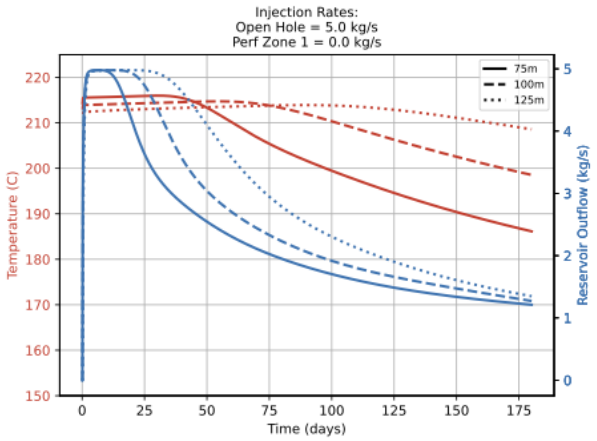

Figure 14. Numerical model results for Case 6. Red lines represent the simulated thermal breakthrough, while the blue lines represent the mass fraction of in-situ reservoir water produced corresponding to conservative fluid transport. The solid line represents the 75m well separation scenario, the long dash the 100m scenario, and the short dash the 125m separation scenario.

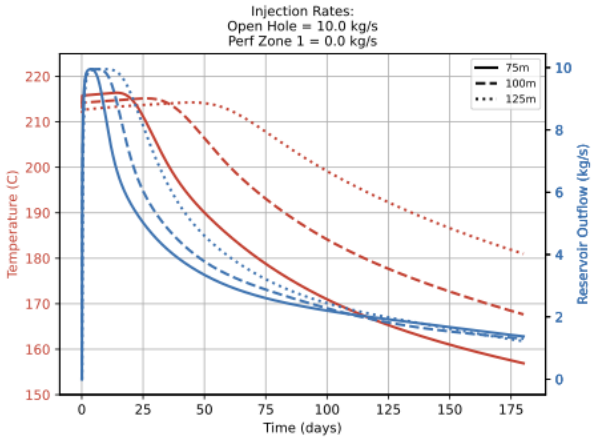

Figure 15. Numerical model results for Case 7. Red lines represent the simulated thermal breakthrough, while the blue lines represent the mass fraction of in-situ reservoir water produced corresponding to conservative fluid transport. The solid line represents the 75m well separation scenario, the long dash the 100m scenario, and the short dash the 125m separation scenario.

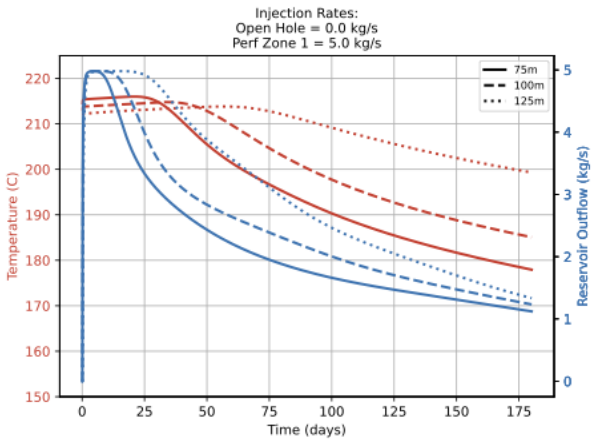

Figure 16. Numerical model results for Case 8. Red lines represent the simulated thermal breakthrough, while the blue lines represent the mass fraction of in-situ reservoir water produced corresponding to conservative fluid transport. The solid line represents the 75m well separation scenario, the long dash the 100m scenario, and the short dash the 125m separation scenario.

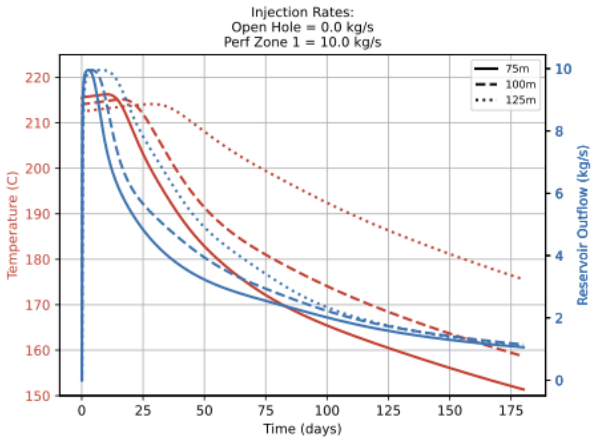

Figure 17. Numerical model results for Case 9. Red lines represent the simulated thermal breakthrough, while the blue lines represent the mass fraction of in-situ reservoir water produced corresponding to conservative fluid transport. The solid line represents the 75m well separation scenario, the long dash the 100m scenario, and the short dash the 125m separation scenario.

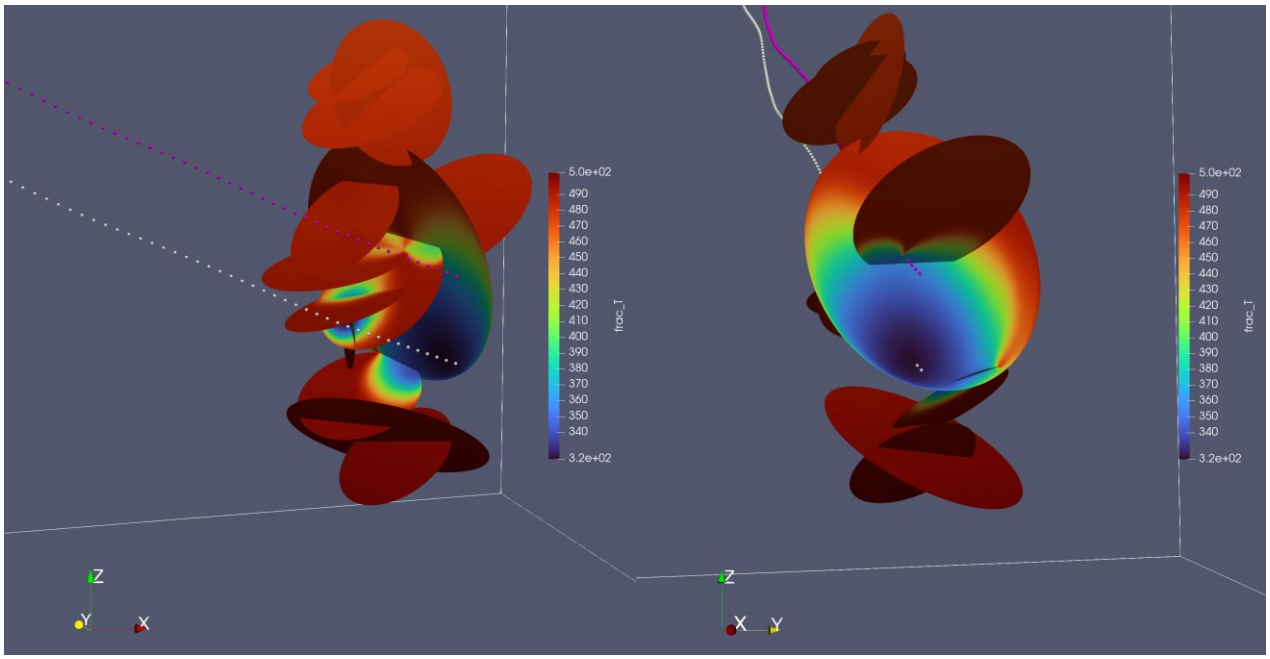

Figure 18. Three-dimensional view of the temperature distribution in the fracture domain after 6 months of injection. Case 1, 75m separation scenario shown. The temperature distribution in the fracture zone is complex owning to the multiple source and sink locations. Temperature shown in Kelvin.

3.2 XSite models

Water circulation between wells 16A and 16B was simulated using a coupled THM model (Detournay et al. 2022). In this model, heat advection with flowing fluid in fractures, convective heat transfer between fluid and rock and heat conduction in the rock are simulated coupled with fluid flow in discrete fractures and mechanical model of rock deformation. For computational efficiency it is assumed that the flow model is continuously in steady state and the mechanical model is in equilibrium. Those assumptions are reasonable considering that characteristic time scales of the fracture flow and mechanical models are much smaller than the characteristic time scale of heat conduction (which is relatively slow process). The model is advanced in time using heat transport processes, heat advection by flowing fluid and heat conduction. At time interval that is sufficiently small, the model is re-equilibrated mechanically for thermally induced stress changes. Subsequently, the flow model is simulated to achieve new steady state corresponding to changed apertures (i.e., permeability). The flow rates from the steady state flow model are used in the advection model in the next thermal step.

The model is used to simulate water circulation from well 16A to well 16B. Two locations of well 16B were assumed in the analyses, with sub-horizontal section 100 m and 150 m above the sub-horizontal section of well 16A. It is assumed that fluid percolation takes place only in stimulated pre-existing fractures and created hydraulic fracture (in zone 3) as identified by interpreting the microseismic data. It is assumed that water is injected at 10 kg/s into all three stimulated zones, hydraulically connected along well 16A.

The fluid pressure contours after 80 days of fluid circulation for both cases of well 16B positioning are shown in Figure 19. The pressure required to achieve same flow rate is 3.5 MPa greater for larger spacing of the wells. The contours of fracture aperture after 80 days of water circulation, shown in Figure 20, indicate the effect of secondary stimulation and fracture opening due to rock cooling around the injection well. However, even though the apertures increase around the injection well (16A) the injection pressures and injectivity remain practically the same. These results indicate that cooling of rock might not be very effective in improving injectivity during water circulation.

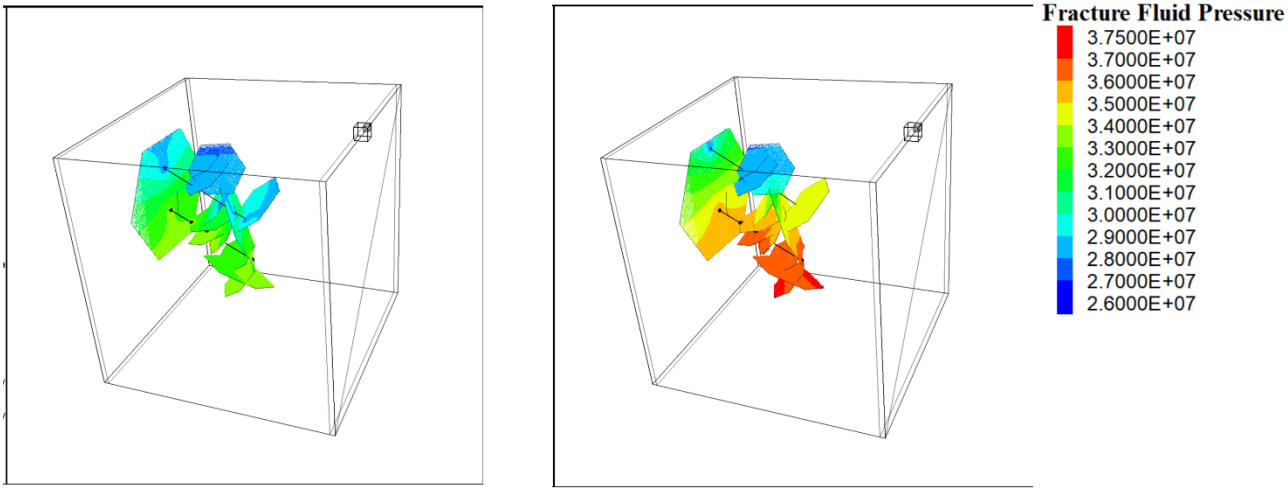

a) 100 m well spacing

b) 150 m well spacing

Figure 19: Fluid pressure (Pa) contours after 80 days of circulation.

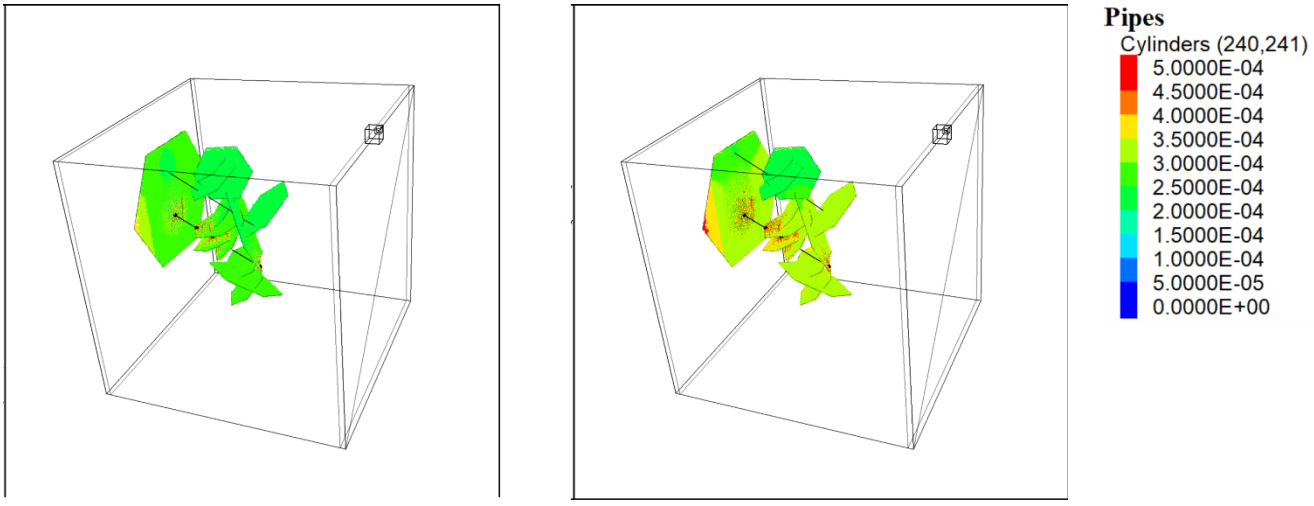

a) 100 m well spacing

b) 150 m well spacing

Figure 20: Fracture aperture (m) contours after 80 days of circulation.

The contours of fluid temperature after 80 days are shown in Figure 21 and histories of produced water temperatures are shown in Figure 22. The results are shown for two cases of well spacing. The entire injected water is recovered from the production well because limited number of fractures are included in the model completely disconnected from rest of the DFN. This model is unconservative because it does not include any risk of losing some of the injected fluid. The temperature of the produced water is calculated by volume averaging temperatures of water produced from all fractures intersected by the production well. The temperature drops for both cases of well spacing are relatively large and, as expected, greater for closer spacing. In 80 days, temperature of produced water drops 31°C and 17°C, for 100 m

and 150 m well spacing, respectively. The rock temperature contours, shown in vertical cross-section along the wells in Figure 23, are consistent with the temperature histories of produced water. Only a "skin" of rock cools along the fracture length between wells 16A and 16B. The skin cooling also explains relatively small effect of temperature changes on fracture apertures and injectivity.

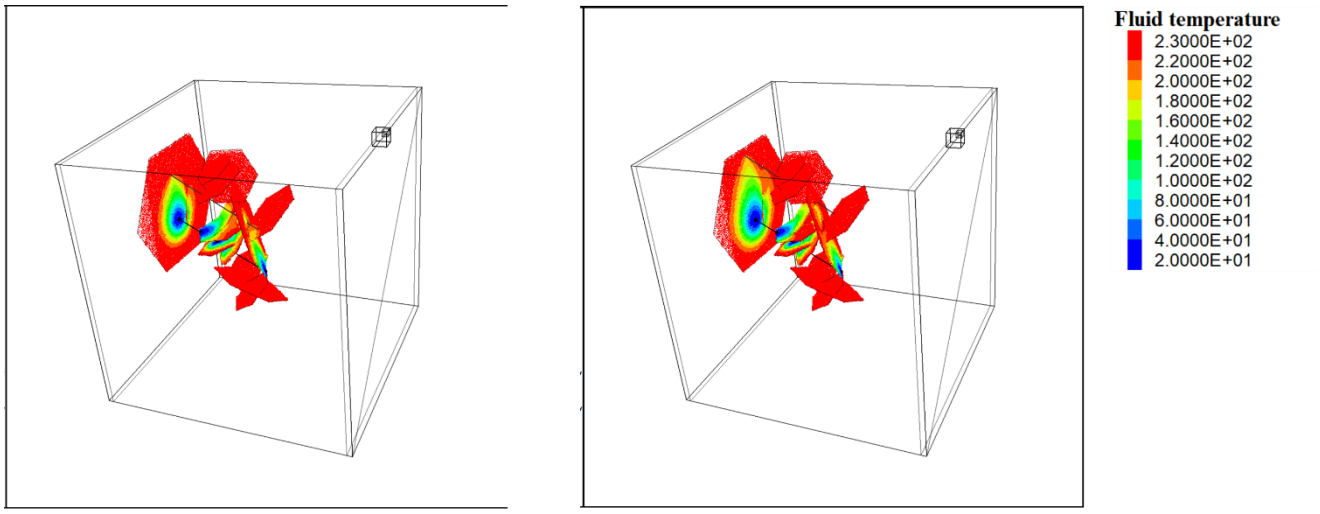

a) 100 m well spacing

b) 150 m well spacing

Figure 21: Fluid temperature (°C) contours after 80 days of circulation.

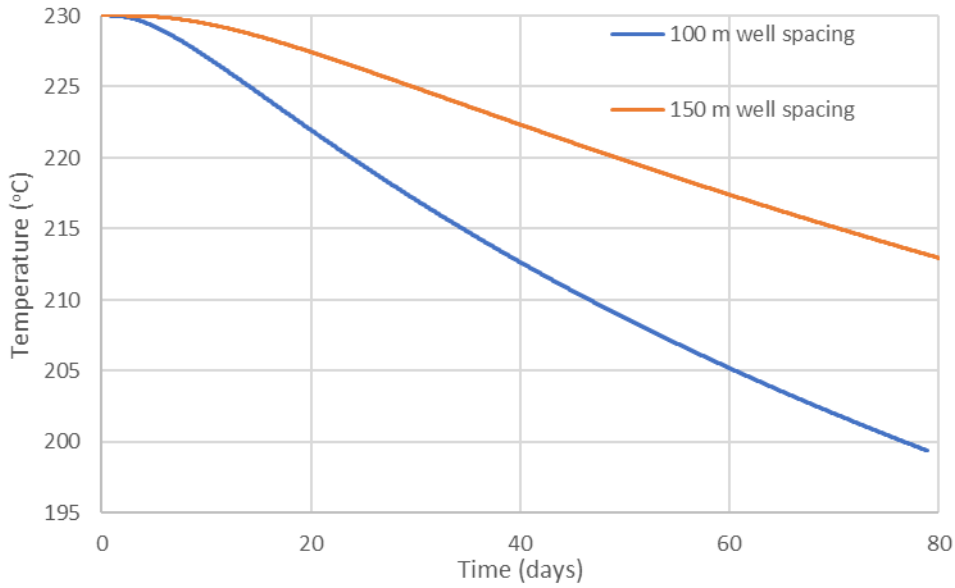

Figure 22: Temperature histories of produced water.

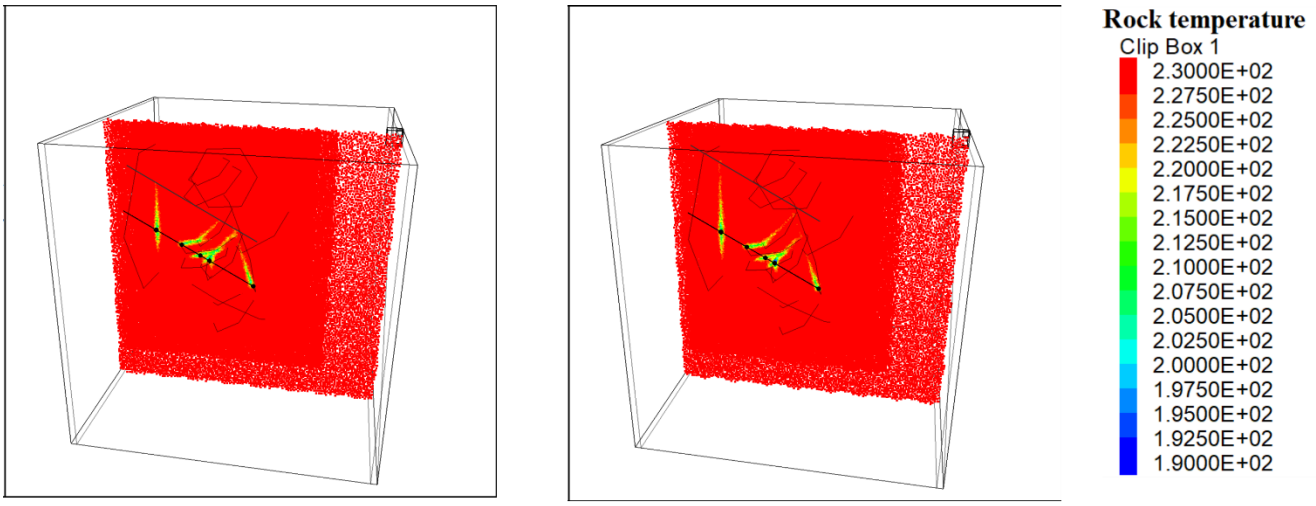

Figure 23: Rock temperature (°C) contours after 80 days of circulation.

4.0 CONCLUSIONS

The paper presented a status update of modeling and simulation activities undertaken to support design decisions for the location and completion options for Well 16B at the Utah FORGE site. A range of injection distribution scenarios were tested to examine potential fluid production trends and times for conservative (pure fluid) and thermal breakthrough.

Thermal breakthrough as early at only a few days were prediction for an injection rate of 100 kg/s, with lower flow rates prediction thermal arrivals between 16 and 50 days. Tracer/conservative breakthrough occurred as early as 7 days for injection rate of 10 kg/s.

This analysis is on-going, with additional simulation cases and numerical complexity currently underway.

REFERENCES

Damjanac, B., Detournay, C., Cundall, P. 2020. Numerical Simulation of Hydraulically Driven Fractures. In: Shen, B., Stephansson, O., Rinne, M. (eds) Modelling Rock Fracturing Processes. Springer, Cham. https://doi.org/10.1007/978-3-030-35525-8_20

Detournay, C., Damjanac, B., Torres, M., Cundall, P., Ligocki, L., and Gil, I., Heat advection and forced convection in a lattice code – Implementation and geothermal applications, Rock Mechanics Bulletin, Volume 1, Issue 1, (2022), 100004, ISSN 2773-2304, https://doi.org/10.1016/j.rockmb.2022.100004.

Finnila, A., Doe, T., Podgorney, R., Damjanac, B., and Xing, P. "Revisions to the Discrete Fracture Network Model at Utah FORGE Site." GRC Transactions, Vol 45 (2021).

Lindsay, A. D., Gaston, D. R., Permann, C. J., Miller, J. M., Andrš, D., Slaughter, A. E., Kong, F., Hansel, J., Carlsen, R. W., Icenhour, C., Harbour, L., Giudicelli, G. L., Stogner, R. H., German, P., Badger, J., Biswas, S., Chapuis, L., Green, C., Hales, J., … Wong, C. (2022). 2.0 - MOOSE: Enabling massively parallel multiphysics simulation. *SoftwareX*, *20*, 101202. https://doi.org/https://doi.org/10.1016/j.softx.2022.101202

Podgorney, R., Finnila, A., Simmons, S., McLenna, J.: A Reference Thermal-Hydrologic-Mechanical Native State Model of the Utah FORGE Enhanced Geothermal Site, Energies 2021, 14, 4758.

Podgorney, R.; Huang, H.; Lu, C.; Gaston, D.; Permann, C.; Guo, L.; Andrs, D. Falcon: A Physics-Based and Massively Parallel and Fully-Coupled, Finite Element Model for Simultaneously Solving Multiphase Fluid Flow, Heat Transport, and Rock Deformation for Geothermal Reservoir Simulation; Technical Report INL/EXT-11e23351; Idaho National Laboratory: Idaho Falls, ID, USA, 2014.

University of Utah Seismograph Stations. (2022). Seismic Data from the Well 16A(78)-32 Stimulation April, 2022 [data set]. Retrieved from https://dx.doi.org/10.15121/1879450.

Willis, B and R. Podgorney, 2023, Thermal Hydraulics Evaluation of Fluid Flow Distribution in a Multi-Stage Stimulated Enhanced Geothermal System Wellbore at the Utah FORGE Site, PROCEEDINGS, 48th Workshop on Geothermal Reservoir Engineerin Stanford University, Stanford, California, February 6-8, 2023 SGP-TR-224

WSP: FracMan® Reservoir Edition, version 8.1 Discrete Fracture Network Simulator, (2022).

WSP Golder. (2022). Utah FORGE Well 16A(78)-32 Stimulation DFN Fracture Plane Evaluation and Data [data set]. Retrieved from https://dx.doi.org/10.15121/1901784.

Xia, Y., Plummer, M., Mattson, E., Podgorney, R., Ghassemi, A.: Design, Modeling, and evaluation of a double heat extraction model in enhanced geothermal systems, Renewable Energy, 105, (2017), 232-247.

Xia, Y.; Podgorney, R.: Falcon: Finite Element Geothermal Reservoir Simulation Code. Available online: https://mooseframework.inl.gov/falcon/ (accessed on 1 August 2021).

.